

# Microinjection of Anti-coilin Antibodies Affects the Structure of Coiled Bodies

Fátima Almeida,\* Rainer Saffrich,<sup>‡</sup> Wilhelm Ansorge,<sup>‡</sup> and Maria Carmo-Fonseca\*

\*Institute of Histology and Embryology, Faculty of Medicine, University of Lisbon, 1699 Lisboa Codex, Portugal; and <sup>‡</sup>European Molecular Biology Laboratory, D-69117 Heidelberg, Germany

**Abstract.** The coiled body is a distinct subnuclear domain enriched in small nuclear ribonucleoprotein particles (snRNPs) involved in processing of pre-mRNA. Although the function of the coiled body is still unknown, current models propose that it may have a role in snRNP biogenesis, transport, or recycling. Here we describe that anti-coilin antibodies promote a specific disappearance of the coiled body in living human cells, thus providing a novel tool for the functional analysis of this structure. Monoclonal antibodies (mAbs) were raised against recombinant human coilin, the major structural protein of the coiled body. Four mAbs are shown to induce a progressive disappearance of coiled bodies within ~6 h after microinjection into the nucleus of HeLa cells. After their disappearance, coiled bodies are not seen to re-form, although injected cells remain

viable for at least 3 d. Epitope mapping reveals that the mAbs recognize distinct amino acid motifs scattered along the complete coilin sequence. By 24 and 48 h after injection of antibodies that promote coiled body disappearance, splicing snRNPs are normally distributed in the nucleoplasm, the nucleolus remains unaffected, and the cell cycle progresses normally. Furthermore, cells devoid of coiled bodies for ~24 h maintain the ability to splice both adenoviral pre-mRNAs and transiently overexpressed human  $\beta$ -globin transcripts. In conclusion, within the time range of this study, no major nuclear abnormalities are detected after coiled body disappearance.

**Key words:** coiled body • p80-coilin • splicing • spliceosomal snRNPs • nucleolus

**T**HE intranuclear structure that is now known as the coiled body was first described in 1903 by the neurocytologist Ramon-y-Cajal. Cajal observed that neurons stained with silver contained spherical structures ~0.5  $\mu$ m in diameter which were often associated with nucleoli, and called them nucleolar accessory bodies. Later, electron microscopists have rediscovered the accessory body of Cajal and introduced the name coiled body because when this structure is viewed with the electron microscope it resembles a tangle of coiled threads (Hardin et al., 1969; Monneron and Bernhard, 1969; Hervás et al., 1980).

The next major advance in the study of coiled bodies came with the discovery of patient autoimmune sera that selectively stain these structures and react with a protein of ~80 kD termed p80-coilin (Raska et al., 1990, 1991; Andrade et al., 1991). Anti-coilin antibodies proved to be a very convenient marker for identifying coiled bodies, and data from numerous laboratories indicate that similar or equivalent structures are present in nuclei from plants (Moreno Diaz de la Espina et al., 1980; Beven et al., 1995),

flies (Yannoni and White, 1997), frogs (Gall et al., 1995; Roth, 1995), birds (Ochs et al., 1995), and mammals (for review see Bohmann et al., 1995b).

The gene encoding p80-coilin has been cloned and sequenced (Andrade et al., 1991; Chan et al., 1994; Wu et al., 1994; Carmo-Fonseca et al., 1994). The deduced protein sequence shows no prominent homology to other known proteins, except for the *Xenopus* protein SPH-1 (Tuma et al., 1993). This protein is highly homologous to coilin at both its amino and carboxy termini, but shows much less homology in the internal domain (see Carmo-Fonseca et al., 1994). In the nucleus of amphibian oocytes SPH-1 is localized in spheres that are thought to be equivalent to coiled bodies (for review see Roth, 1995; Gall et al., 1995). The coilin sequence includes two motifs at amino acid positions 107–112 and 181–198 that closely match the consensus sequence of the simple and bipartite nuclear localization sequence (NLS)<sup>1</sup>, respectively (Bohmann et al., 1995a). Mutational analysis data are consistent with both

Address all correspondence to M. Carmo-Fonseca, Institute of Histology and Embryology, Faculty of Medicine, Av. Prof. Egas Moniz, 1699 Lisboa Codex, Portugal. Tel.: (351) 1 7934340. Fax: (351) 1 7951780. E-mail: hcarmo@fm.ul.pt

1. *Abbreviations used in this paper.* Ad2, adenovirus type 2; BrdU, bromodeoxyuridine; BrUTP, 5-bromo-2'-uridine-5'-triphosphate; Cy5, indodicarbocyanine; MLP, major late promoter; NLS, nuclear localization signal; snoRNA, small nucleolar RNA; snRNP, small nuclear ribonucleoprotein.

NLS motifs having a function in nuclear import. However, they may contribute differentially to the transport and are not sufficient to target coilin to the coiled body (Bohmann et al., 1995a). The protein sequence of p80-coilin include a high percentage of serine residues, several of which are phosphorylated in vivo (Carmo-Fonseca et al., 1993). In a more recent mutational analysis, a single amino acid change at position 202, converting the wild-type sequence from serine to aspartate (which simulates a constitutively phosphorylated serine), was shown to cause the disappearance of coiled bodies and a redistribution of coilin to intranucleolar domains (Lyon et al., 1997). Similar results were observed after exposure of cells to the specific Ser/Thr protein phosphatase inhibitor, okadaic acid, suggesting that protein dephosphorylation is required for normal coiled body assembly (Lyon et al., 1997).

In addition to p80-coilin, other components of the coiled body include the U1, U2, U4/U6, and U5 small nuclear ribonucleoprotein particles (snRNPs) involved in splicing of pre-mRNA (Carmo-Fonseca et al., 1991a, 1992); the U7 snRNA required for 3' end processing of histone mRNA (Frey and Matera, 1995); the nucleolar protein fibrillarin (Raska et al., 1990, 1991) and the fibrillarin-associated U3 and U8 small nucleolar RNAs (snoRNAs) involved in processing of pre-rRNA (Wu et al., 1993; Bauer et al., 1994; Jiménez-García et al., 1994); nucleolar proteins Nopp140 and NAP57 (Meier and Blobel, 1994) and ribosomal protein S6 (Jiménez-García et al., 1994). Finally, the coiled body contains a number of kinases, namely the cdk-activating kinase associated with the transcription factor TFIIF, the cAMP-dependent protein kinase, and the double-stranded RNA-activated protein kinase, DAI (Jordan et al., 1997).

After the initial discovery that coiled bodies are highly enriched in spliceosomal snRNPs, it was proposed that they may be functionally related to splicing (Carmo-Fonseca et al., 1991a). However, the coiled body does not contain essential non-snRNP protein-splicing factors, such as SR proteins and U2AF65 (Carmo-Fonseca et al., 1991b; Gama-Carvalho et al., 1997), and does not accumulate nascent transcripts (Huang et al., 1994; Rebelo et al., 1996; Jordan et al., 1997). Thus, it is unlikely that coiled bodies represent major sites of pre-mRNA splicing. Consequently, it was suggested that the coiled body may be involved in some aspect of snRNP biogenesis, transport, or recycling (Lamond and Carmo-Fonseca, 1993; Bohmann et al., 1995b; Gall et al., 1995).

In the present work we have raised a family of mAbs that react with distinct amino acid motifs scattered along the coilin protein. Upon microinjection of HeLa cells into the nucleus, four distinct antibodies are shown to promote the disappearance of coiled bodies, thus providing a novel tool to investigate the function of this subnuclear compartment.

## Materials and Methods

### Production of mAbs

Two partial human p80-coilin cDNAs were cloned into the His6-tag vectors pRSET B and pRSET A (Invitrogen, Leek, The Netherlands). The corresponding His-coilin fusion proteins were expressed in *Escherichia*

*coli* and purified using an Ni-NTA agarose affinity column (Quiagen, Hilden, Germany), as previously described (Bohmann et al., 1995a). For immunizations, 6-wk-old female BALB/c mice were used. Five animals were injected with the amino-terminal 127 amino acids of coilin, and another five animals were immunized with the carboxy-terminal 389 amino acids. The fusion proteins were diluted in 0.1 M sodium phosphate buffer, pH 8, to a concentration of 0.2 mg/ml, emulsified with Freund's adjuvant (Difco Laboratories, Detroit, MI), and then injected intraperitoneally. Mice were boosted twice at 3-wk intervals and test bleeds were taken. The sera were screened by immunofluorescence and immunoblotting. The spleen cells from the two mice with higher antisera titers were fused with Ag8.653 myeloma cells and hybrids were selected as described by Harlow and Lane (1988). After 10 d, hybridoma supernatants were tested for reactivity by immunofluorescence and immunoblotting. Of 456 fusion wells, 216 tested positive and six were successfully cloned by limiting dilution on microtiter plates. These hybridoma cell lines were used to induce a peritoneal tumor in pristane (Carl Roth, Karlsruhe, Germany) primed adult female mice (Harlow and Lane, 1988). Ascitic fluid was collected and immunoglobulin class, subclass, and light chain type was determined using a mouse-hybridoma subtyping kit (Boehringer Mannheim, Mannheim, Germany). All mAbs were purified from ascitic fluid by DEAE Affi-Gel blue chromatography (Bio-Rad Laboratories, Munich, Germany) as described (Bruck et al., 1982), and subsequently concentrated by ultrafiltration on Ultrafree-15 membranes (Millipore Corporation, Waters Chromatography, Bedford, MA). Purified mAbs were conjugated to lissamine rhodamine B200 sulfonylechloride (Polysciences, Warrington, PA) by using standard procedures.

### Generation and Expression of Full-length and Mutant p80-Coilin Constructs

Deletion mutants were derived from pKH8 and pBS751.2A (Bohmann et al., 1995a) by using appropriate restriction enzyme sites. Plasmid pKH8 encodes the carboxy-terminal 389 amino acids of coilin, whereas pBS751.2A contains the full-length coding region of the protein. Both the full-length and truncated forms of p80-coilin were expressed in *E. coli* and purified as His-tag fusion proteins by Ni-NTA affinity chromatography.

### Cell Culture

HeLa cells were grown as monolayers in minimum essential medium (MEM) with Earle's Salts supplemented with 2 mM L-glutamine, 1% MEM nonessential amino acids, 50 IU/ml penicillin and 50 mg/ml streptomycin, and 10% fetal calf serum (GIBCO BRL, Paisley, Scotland, UK). Infection with adenovirus type 2 (Ad2) was performed as described (Rebelo et al., 1996).

### SDS-PAGE and Immunoblotting

HeLa cells were harvested by trypsinization and crude nuclei were isolated as described (Jordan et al., 1996). Cells and isolated nuclei were mixed with SDS-PAGE sample buffer (62.5 mM Tris-HCl pH 6.8, 2% SDS, 5%  $\beta$ -mercaptoethanol, 10% glycerol, and 0.01% bromophenol blue) containing 200 U/ml benzoylase (Sigma Chemical Co., St. Louis, MO), incubated for 15 min at room temperature (to digest DNA) and then boiled for 5 min. Purified His-coilin fusion proteins were directly boiled in SDS-PAGE sample buffer. Proteins were separated on either 8, 10, 12, or 15% acrylamide gels and transferred to nitrocellulose membranes using a semi-dry electrotransfer apparatus (Bio-Rad Laboratories, Hercules, CA). The membranes were blocked and washed with 2% nonfat milk powder in PBS. The blots were incubated for 1 h with primary antibodies diluted in washing buffer, washed three times for 10 min each in the same buffer, incubated for 1 h with secondary antibodies conjugated to horseradish peroxidase (Bio-Rad Laboratories) and developed using a chemiluminescence reaction (enhanced chemiluminescence; Amersham Int., Buckinghamshire, England, UK).

### Immunofluorescence

For indirect immunofluorescence cells were grown on  $10 \times 10$ -mm glass coverslips. The cells were washed twice in PBS, fixed with 3.7% formaldehyde (freshly prepared from paraformaldehyde) in PBS for 10 min at room temperature, and subsequently permeabilized with 0.5% Triton X-100 in PBS for 15 min at room temperature. Alternatively, cells were first per-

meabilized with 0.5% Triton X-100 in CSK buffer (100 mM NaCl, 300 mM sucrose, 10 mM Pipes, 3 mM MgCl<sub>2</sub>, 1 mM EGTA, pH 6.8; Fey et al., 1986) containing 0.1 mM PMSF for 1 min on ice, and subsequently fixed with 3.7% formaldehyde in CSK buffer, for 10 min at room temperature. After fixation and permeabilization the cells were rinsed in PBS containing 0.05% Tween-20 (PBS-Tw), incubated for 30 min with primary antibodies diluted in PBS, washed in PBS-Tw, and then incubated for 30 min with the appropriate secondary antibodies conjugated to fluorescein (FITC), Texas red, or indodicarbocyanine (Cy5) (Jackson Immuno-Research Laboratories, West Grove, PA). Finally, the coverslips were mounted in VectaShield (Vector Laboratories, Peterborough, UK) and sealed with nail polish.

### Visualization of Replication and Transcription Sites

For the visualization of replication sites, 50  $\mu$ M bromodeoxyuridine (BrdU; Boehringer Mannheim) was added to the culture medium for either 2 or 24 h. To detect the incorporated BrdU, the cells were permeabilized with 0.5% Triton X-100 and fixed in formaldehyde as described above. The cellular DNA was denatured by incubation in 1.5 M HCl for 10 min at room temperature. Detection of BrdU-DNA was performed by indirect immunofluorescence using purified sheep anti-BrdU polyclonal antibody (Biosdesign International, Kennebunk, ME) and a secondary antibody coupled to fluorescein.

For the detection of nucleoplasmic transcription 5-bromo-2'-uridine-5'-triphosphate (BrUTP, 5  $\mu$ M of solution; Sigma Chemical Co.) was microinjected into the cytoplasm of HeLa cells. The cells were further incubated for 10 min at 37°C, permeabilized with 0.5% Triton X-100, and fixed in formaldehyde as described above. The incorporated bromo-uridine was detected using a monoclonal antibody directed against BrdU (Boehringer Mannheim) and a secondary antibody labeled with fluorescein.

### In Situ Hybridization

For in situ hybridization, cells were fixed with 3.7% formaldehyde in CSK buffer for 10 min at room temperature and subsequently permeabilized with 0.05% SDS in 100 mM Tris-HCl, pH 7.5, 150 mM NaCl, 12.5 mM EDTA, for 5 min. Detection of spliced transcripts was performed using synthetic oligonucleotide probes, as previously described (Zhang et al., 1994; Bridge et al., 1996). Detection of U2 snRNA, U3 snoRNA, and 28S rRNA was performed using biotinylated 2'-O-allyl oligoribonucleotide probes, as previously reported (Carmo-Fonseca et al., 1992).

### Confocal Microscopy

Samples were analyzed with the laser-scanning microscope LSM410 (Carl Zeiss, Inc., Thornwood, NY). Argon ion (48-nm), HeNe (54-nm), and Kr (63-nm) lasers were used to excite FITC, Texas red, and Cy5 fluorescences, respectively.

### Microinjections and Live Cell Observations

For microinjection experiments, cells were grown on either 10  $\times$  10-mm glass coverslips or CELlocate coverslips (Eppendorf Scientific, Hamburg, Germany). Micropipettes obtained from Clark Electromedical Instruments (Pangbourne, UK) were freshly prepared on a P-87 puller (Sutter Instruments, Novato, CA) and microinjections were performed using either an Eppendorf microinjector 5242 (Eppendorf Scientific, Inc., Hamburg, Germany) or the AIS system (Ansoarg and Pepperkok, 1988). Purified mAbs were microinjected at concentrations ranging between 2.5 and 5 mg/ml. Plasmid DNA was microinjected at 0.1 mg/ml. For live cell observations, the cells were grown in glass bottom microwell dishes (MatTek Corporation, Ashland, MA) placed in a temperature-controlled chamber on the stage of an inverted microscope (Carl Zeiss, Inc., Oberkochen, Germany). The medium in the dish was overlaid with mineral oil to slow evaporation. Images were acquired with a Photometrics (Tucson, AZ) cooled slow scan charge-coupled device camera CH250 with a CE200A camera control unit, using a 63 $\times$ , 1.4 NA Plan Apo oil immersion lens (Carl Zeiss, Inc.). The system included motorized shutters and filter wheels with a SUN Sparstation 10/41 providing automated time-lapse data collection using the KHOROS software, as previously described (Herr et al., 1993).

## Results

### Specificity of Anti-coilin mAbs

To obtain monoclonal antibodies, hybridomas were derived by fusion of the mouse myeloma cell line Ag8.653 with spleen cells from Balb/c mice immunized with recombinant human coilin. Six clones (designated  $\delta$ , p $\delta$ ,  $\gamma$ ,  $\pi$ , o, and  $\phi$ ) were isolated. The antibodies secreted by clones  $\delta$ , p $\delta$ , o, and  $\phi$  are of the IgG1 class, whereas mAb- $\gamma$  is IgG2b and mAb- $\pi$  is IgG2a (Table I). Immunoblot analysis reveals that all mAbs recognize a band of  $\sim$ 80 kD in HeLa protein extracts (Fig. 1, A and B). Clones  $\pi$  and  $\delta$  react specifically with p80-coilin, whereas the other clones cross-react with additional peptides. In addition to coilin, the mAbs o and  $\gamma$  recognize a major cytoplasmic protein band of  $\sim$ 140 kD, mAb- $\phi$  strongly reacts with a nuclear

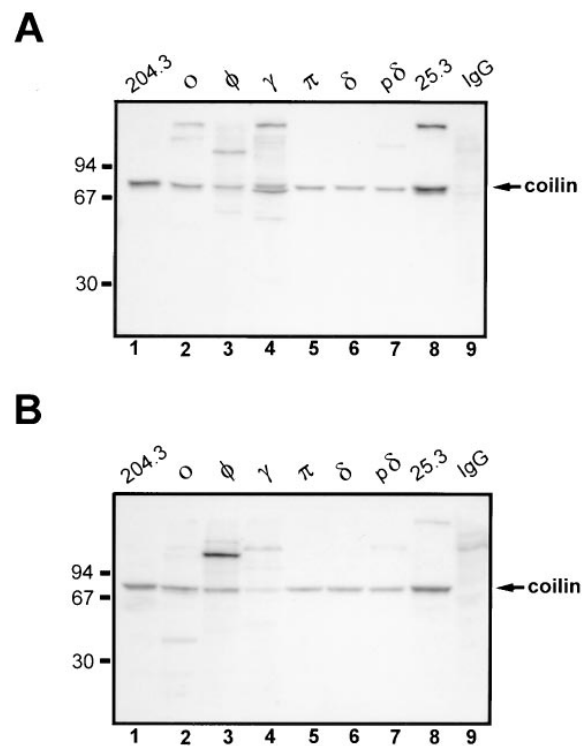


**Figure 1.** Immunoblot analysis of anti-coilin mAbs. An 8% acrylamide gel was loaded with either total protein extract from HeLa cells ( $2 \times 10^5$  cells/well) (A) or a protein extract from isolated HeLa cell nuclei ( $10^6$  cell equivalents/well) (B). Immunoblot analysis was performed using the following antibodies: rabbit antiserum 204.3 (diluted 1:20,000) (lane 1); mAb-o (25  $\mu$ g/ml purified IgG) (lane 2); mAb- $\phi$  (10  $\mu$ g/ml purified IgG) (lane 3); mAb- $\gamma$  (25  $\mu$ g/ml purified IgG) (lane 4); mAb- $\pi$  (5  $\mu$ g/ml purified IgG) (lane 5); mAb- $\delta$  (0.08  $\mu$ g/ml purified IgG) (lane 6); mAb-p $\delta$  (15  $\mu$ g/ml purified IgG) (lane 7); mouse antiserum 25.3 (diluted 1:5,000) (lane 8); and nonspecific polyclonal mouse IgG (5  $\mu$ g/ml purified IgG) (lane 9). Due to significant differences in the binding affinity of each mAb, different antibody concentrations were used in order to produce a signal of similar intensity. Antiserum 25.3 derives from the mouse used to produce hybridomas  $\phi$ ,  $\gamma$ ,  $\pi$ ,  $\delta$ , and p $\delta$ . Nonspecific mouse IgG was purchased from Sigma Chemical Co. Molecular mass markers (kD) are indicated on the left.

A

	$\delta$	$p\delta$	$\gamma$	$\pi$	$o$	$\phi$
1-576	+	+	+	+	+	+
1-127	-	-	-	-	+	-
187-576	+	+	+	+	-	+
187-481	+	+	+	-	-	+
187-291	-	-	-	-	-	+
292-576	+	+	+	+	-	-
292-481	+	+	+	-	-	-
292-362	-	-	+	-	-	-
363-576	+	+	-	+	-	-
363-481	+	+	-	-	-	-
482-576	-	-	-	-	-	-

B

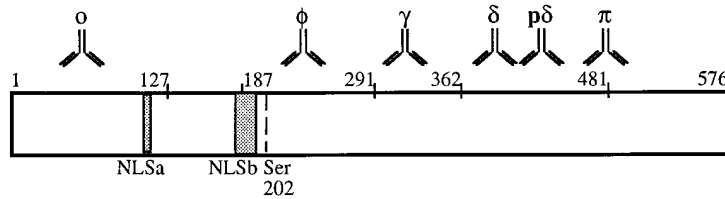


Figure 2. Epitope mapping of mAbs. (A) Diagram showing the reactivity of each mAb with the full-length coilin and different deletion mutants of the protein, as determined by immunoblot analysis. The data show that the epitopes recognized by mAbs  $o$ ,  $\phi$ , and  $\gamma$  map between amino acids 1–127, 187–291, and 292–362, respectively. The mAbs  $\delta$  and  $p\delta$  react with epitopes located between acids 363 and 481. The mAb- $\pi$  recognizes either an epitope localized around amino acids 481–482, or a conformational epitope present in the coilin mutant encompassing amino acids 363–576, but absent from the mutants encompassing amino acids 363–481 and 482–576. (B) Diagram showing the mapped epitopes ( $\Upsilon$ ) in relation to the complete coilin sequence. Hatched regions depict the two motifs that closely match the consensus sequence of simple and bipartite nuclear localization sequences, NLSa and NLSb, respectively (Bohmann et al., 1995a). The diagram also depicts the position of serine 202. Conversion of this amino acid residue into aspartate causes the disappearance of coiled bodies and a redistribution of coilin to intranucleolar domains (Lyon et al., 1997).

protein of  $\sim 110$  kD, and mAb- $p\delta$  reveals a minor nuclear protein band of  $\sim 115$  kD. To map the epitopes recognized by each mAb, a series of His-coilin deletion mutants was generated and probed by immunoblot analysis (Fig. 2). From these data we conclude that the different clones react with epitopes distributed along the entire protein sequence. By immunofluorescence all mAbs labeled coiled bodies (Fig. 3 A and data not shown), as previously reported for clone  $\delta$  (Rebello et al., 1996).

### Microinjection of mAbs Affect the Coiled Body Structure

To determine whether the mAbs interfere with coiled bodies in the native environment of the living cell nucleus, each antibody was purified from ascitic fluid and microin-

jected into the nuclei of interphase HeLa cells. The cells were immediately removed from the microscope stage, permeabilized with detergent, fixed, and then incubated with fluorescent secondary antibodies. The time between injection and fixation was  $\sim 20$  min. As shown in Fig. 3 B, injected mAb- $\delta$  binds to coiled bodies within this time period, producing a labeling pattern similar to that obtained by indirect immunofluorescence on fixed cells (Fig. 3 A). In contrast, when cells are observed 24 h after injection of mAb- $\delta$  the coiled bodies are no longer visible (Fig. 3 C), suggesting that binding of mAb- $\delta$  to coilin affects the structure of the coiled body. To further confirm this idea, similar experiments were performed using mAb- $\delta$  preincubated with recombinant coilin protein. Purified mAb- $\delta$  was incubated for 1 h with increasing concentrations of coilin and then used for indirect immunofluorescence on fixed cells. As shown in Fig. 3 D, no signal was detected after incubation of mAb- $\delta$  with a 1:2 molar excess of coilin, indicating that all antigen binding sites had been blocked. The same preparation of neutralized mAb- $\delta$  was then microinjected into the nucleus of HeLa cells. As expected from its inability to bind to endogenous coilin, immediately after injection mAb- $\delta$  appears diffuse throughout the nucleoplasm (Fig. 3 E, also see B). However, there is an additional faint staining of coiled bodies (Fig. 3 E, arrow), implying that in vivo a small fraction of IgG molecules is still able to bind to endogenous coilin. This could be due to a progressive exchange of recombinant coilin by endo-

Table I. Immunoglobulin Class, Subclass, and Light Chain Typing of Anti-coilin mAbs

mAb	Abbreviated name	Ig subtype
1D4- $\delta$	$\delta$	IgG1/k
5P11- $p\delta$	$p\delta$	IgG1/k
1G3- $\gamma$	$\gamma$	IgG2b/k
5P10- $\pi$	$\pi$	IgG2a/k
3W8- $o$	$o$	IgG1/k
4F9- $\phi$	$\phi$	IgG1/k

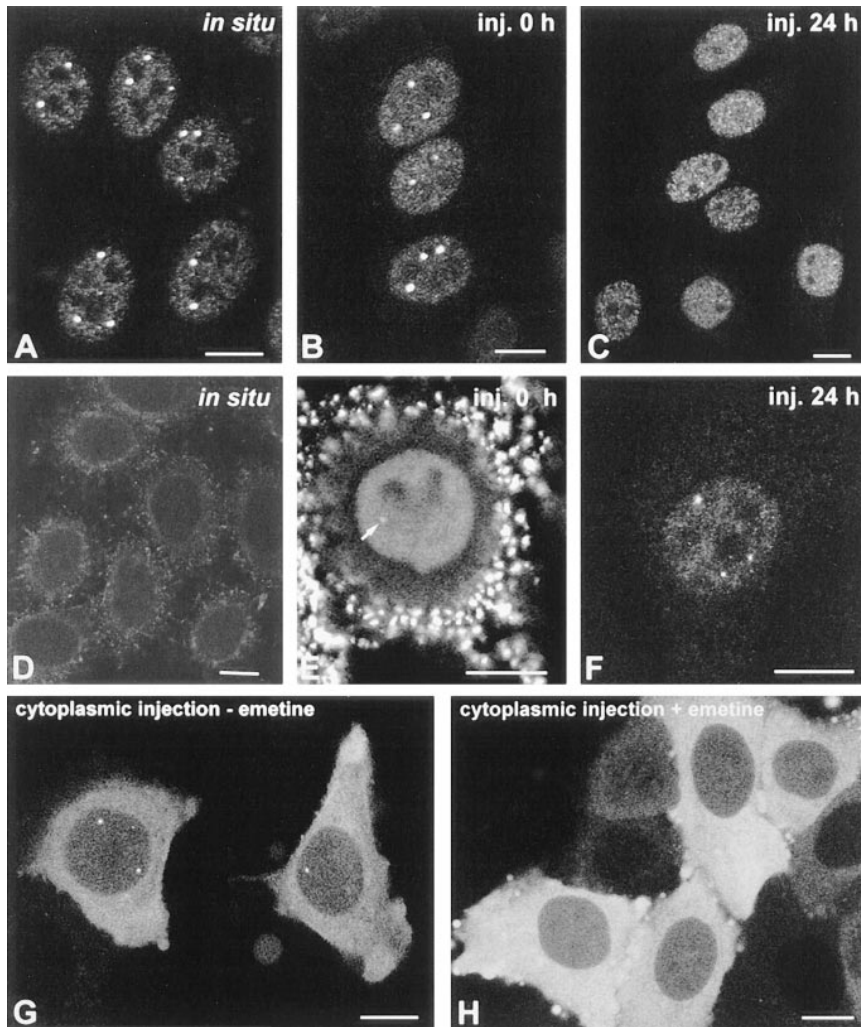


**Figure 3.** Microinjection mAb- $\delta$ . (A) HeLa cells were permeabilized with Triton X-100, fixed with formaldehyde, and then incubated with mAb- $\delta$ . (B and C) HeLa cells were microinjected in the nucleus with mAb- $\delta$ . The cells were then observed immediately (B) or 24 h after injection (C). (D–F) Purified mAb- $\delta$  was incubated for 1 h with 1:2 molar excess of a coilin peptide containing the epitope for this antibody (amino acids 363–481). The neutralized mAb was then used for indirect immunofluorescence on fixed cells (D) or microinjected in the nucleus of living cells (E and F). (E) Immediately after injection the neutralized mAb is diffusely distributed throughout the nucleoplasm with additional staining of a coiled body (arrow). Note the bright pericellular staining which is due to antibody–antigen complexes adsorbed to the cell membrane. (F) 24 h after injection the staining is predominantly concentrated in coiled bodies. (G and H) HeLa cells were microinjected in the cytoplasm with mAb- $\delta$  and observed 1 h after injection. The cells were either nontreated (G) or treated with 10  $\mu\text{g}/\text{ml}$  emetine for 2.5 h before injection (H). Bar, 10  $\mu\text{m}$ .

genous coilin (possibly, the mAb binds to endogenous coilin with higher affinity and/or avidity). Accordingly, 24 h after injection the fluorescent signal is predominantly concentrated in coiled bodies (Fig. 3 F). Most important, these results show that coiled bodies remain intact when cells are microinjected with mAb- $\delta$  neutralized with recombinant coilin.

Although coilin is predominantly concentrated in the coiled body, there is a variable amount of the protein in the nucleoplasm and our previous results suggest that coilin may shuttle between the two pools (Rebelo et al., 1996). We therefore predict that microinjected IgG molecules bind to coilin and may subsequently become incorporated into a coiled body. In fact, coiled bodies are brightly labeled shortly after microinjection of mAb- $\delta$  into the cytoplasm of HeLa cells (Fig. 3 G). Because IgG molecules per se are unable to cross the nuclear pores (Borer et al., 1989), it is most likely that antibody–coilin complexes formed in the cytoplasm are actively translocated to the nucleus (as a consequence of the nuclear localization signals present in the coilin protein) and once in the nucleus, the antibody–coilin complexes are rapidly incorporated into coiled bodies. Consistent with this interpretation, no nuclear staining is observed when mAb- $\delta$  is microinjected

into cells devoid of cytoplasmic coilin due to the presence of a protein synthesis inhibitor (Fig. 3 H).

Injection of mAbs  $\rho\delta$ ,  $\gamma$ ,  $\pi$ ,  $\sigma$ , and  $\phi$  into the nucleus of HeLa cells produce results similar to those observed with mAb- $\delta$ , i.e., rapid staining of the coiled body (Fig. 4, A–C and G–I). Intriguingly, mAbs  $\sigma$  and  $\phi$  stain nucleoli in addition to coiled bodies (Fig. 4, H and I, arrowheads). The intranucleolar staining produced by mAb- $\sigma$  is diffuse (Fig. 4 H, arrowheads), increases in intensity with time after microinjection (Fig. 4 K, arrowhead) and is never observed by indirect immunofluorescence, suggesting that it may reflect an unspecific accumulation of injected antibody in the nucleolus. In contrast, mAb- $\phi$  stains intranucleolar foci (Fig. 4 I, arrowheads) which are also detected by indirect immunofluorescence on fixed cells. Double-labeling experiments using antibodies directed to RNA polymerase I and UBF reveal that these intranucleolar foci correspond to sites of rRNA synthesis (data not shown; Jordan et al., 1996). Interestingly, the epitope recognized by mAb- $\phi$  is adjacent to a critical serine residue (serine 202) which when mutated to aspartate induces the formation of coiled body-like structures inside the nucleolus (Lyon et al., 1997; refer to Fig. 2 B). However, this type of intranucleolar labeling was never observed with anti-coilin

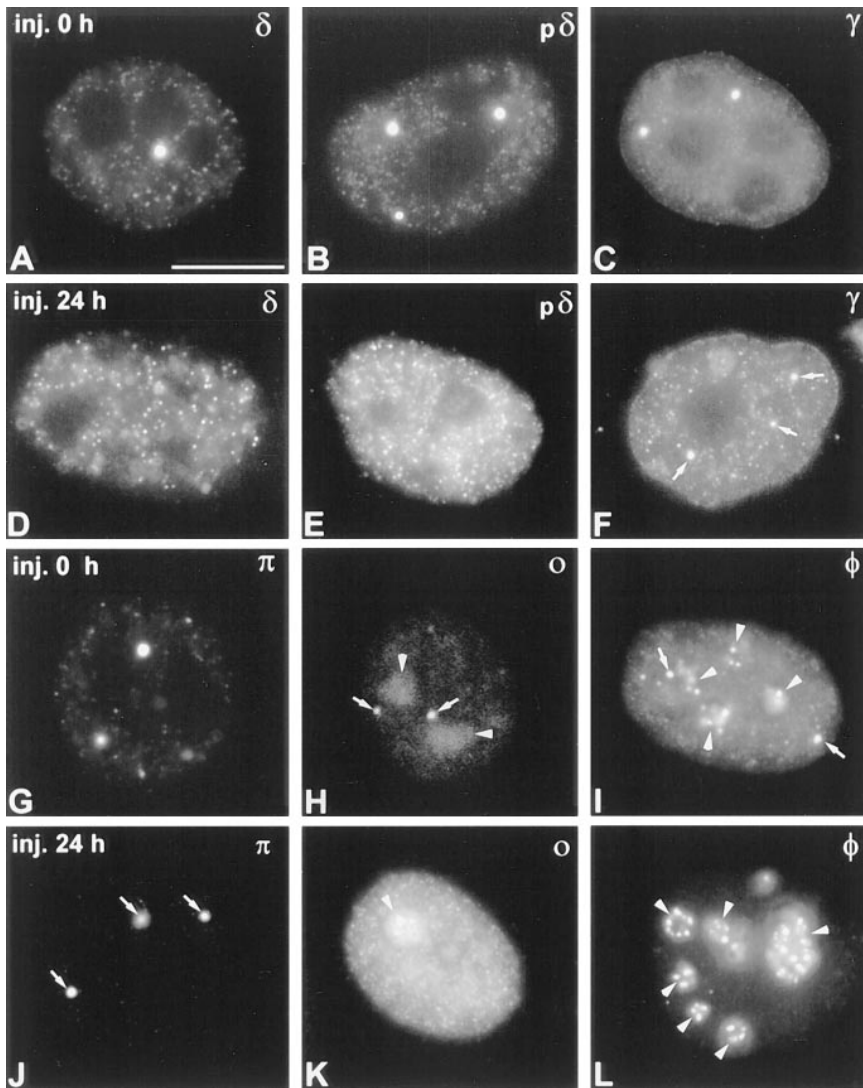


**Figure 4.** The effect of mAb injection on coiled bodies. HeLa cells were microinjected in the nucleus with mAbs  $\delta$  (A and D),  $p\delta$  (B and E),  $\gamma$  (C and F),  $\pi$  (G and J),  $o$  (H and K), and  $\phi$  (I and L). The cells were observed either immediately after injection (A–C, G–I) or 24 h after injection (D–F, J–L). For microscopical observation, the cells were permeabilized with Triton X-100, fixed, and incubated with a secondary antibody coupled to fluorescein. Note that mAbs  $o$  and  $\phi$  label both coiled bodies (arrows) and nucleoli (arrowheads). Bar, 10  $\mu\text{m}$ .

polyclonal antibodies, making it difficult to conclude that it represents an additional localization of coilin within the nucleolus. Rather, it is more likely that mAb- $\phi$  recognizes an epitope common to coilin and another nuclear protein of  $\sim 110$  kD, as revealed by immunoblotting (refer to Fig. 1, A and B, lane 3).

Similar to the results obtained with mAb- $\delta$  (Fig. 4, A and D), when cells are injected with mAb- $p\delta$  and observed 24 h later, coiled bodies are no longer visible (Fig. 4, B and E). Cells injected with mAb- $\gamma$  for 24 h still contain coiled bodies but these appear smaller than in normal cells (Fig. 4, C and F). In contrast, coiled bodies with an apparent normal morphology are observed in cells injected with mAb- $\pi$  for 24 h (Fig. 4, G and J). Finally, injection of mAbs  $o$  and  $\phi$  for 24 h induces the disappearance of coiled bodies without affecting the nucleolar staining (Fig. 4, H, K, I, and L). Noteworthy, by 24 h after injection most mAbs reveal an intense micropunctate staining pattern diffusely distributed throughout the nucleoplasm, excluding the nucleolus (Fig. 4, A and D, B and E, C and F, and H and K). This effect is not observed with mAb- $\pi$ , which

stains predominantly coiled bodies at both 0 and 24 h after injection (Fig. 4, G and J), and mAb- $\phi$ , which labels intranucleolar foci (Fig. 4, I and L).

Although coilin microfoci become more prominent after the disappearance of coiled bodies, similar structures are present in nontreated cells and we have previously demonstrated that at the electron microscopy level they correspond to microspherules of  $\sim 0.05$   $\mu\text{m}$  in diameter (Rebello et al., 1996). Furthermore, we show here that neither coiled bodies nor coilin microfoci colocalize with sites of incorporation of brominated UTP, indicating that they do not correspond to transcription sites (Fig. 5, A and B).

To further characterize the effect of microinjected antibodies on the coiled body, a quantitative analysis was performed. Each mAb was injected into the nuclei of interphase HeLa cells and at 0, 6, and 24 h after injection the cells were fixed, incubated with fluorescein-conjugated secondary antibodies, and then double-labeled with a rabbit anti-coilin antiserum (204.3) detected using Texas red fluorescence. For each time point, the proportion of injected cells with coiled bodies was estimated and the val-

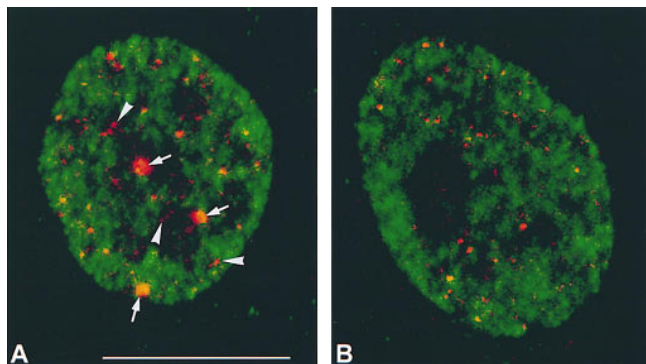


**Figure 5.** Coilin does not colocalize with transcription sites. (A) HeLa cells were microinjected with Br-UTP in the cytoplasm, fixed, and then immunolabeled with mAb- $\pi$ . The sites of incorporated Br-uridine are stained green and the sites containing coilin are stained red. Note that coilin is present both in coiled bodies (arrows) and in numerous nucleoplasmic microfoci (arrowheads). (B) HeLa cells were injected in the nucleus with mAb- $\delta$ . 24 h later the cells were reinjected in the cytoplasm with Br-UTP. Note that the coilin microfoci (stained red) do not colocalize with transcription sites (stained green). Bar, 10  $\mu$ m.

ues at time zero were taken as reference (Fig. 6). The results show that immediately after injection, the proportion of injected cells containing coiled bodies identified by antiserum 204.3 was similar to that of noninjected cells. At 6 and 24 h after injection, the proportion of noninjected cells containing coiled bodies remained unaltered, whereas injected cells showed significant changes. The mAbs  $\delta$ ,  $\alpha$ , and  $\phi$  induce a drastic disappearance of coiled bodies. The mAb  $p\delta$  also reduces the proportion of cells with coiled bodies, although less efficiently than the previous ones. The mAb- $\gamma$  induces a slight decrease in the proportion of injected cells containing coiled bodies at 6 h after injection, but this value remains roughly unchanged by 24 h after injection. In striking contrast with these results, mAb- $\pi$  causes an increase in the relative numbers of injected cells containing coiled bodies.

Importantly, the morphological patterns produced by each mAb at 24 h after injection are maintained up to 3 d, indicating that within this time period, the antibodies are not lethal to the cells and remain stable in the nucleus. Furthermore, addition of BrdU to the culture medium of cells injected for 24–48 h with either mAb- $\delta$  or mAb- $\pi$  indicates that DNA synthesis and mitosis are occurring at approximately the same rates among injected and noninjected cells (data not shown).

In conclusion, we have produced monoclonal antibodies which, depending on their binding sites on coilin, are able to differentially interfere with the structure of the coiled body in vivo.

### Visualization of Coiled Bodies in Living Cells

To clarify the mechanisms by which the anti-coilin antibodies are affecting the coiled body, images of live cells were recorded at 20–30-min intervals after injection of mAbs coupled to rhodamine.

Injection of rhodamine-labeled mAb- $\pi$  into the nucleus

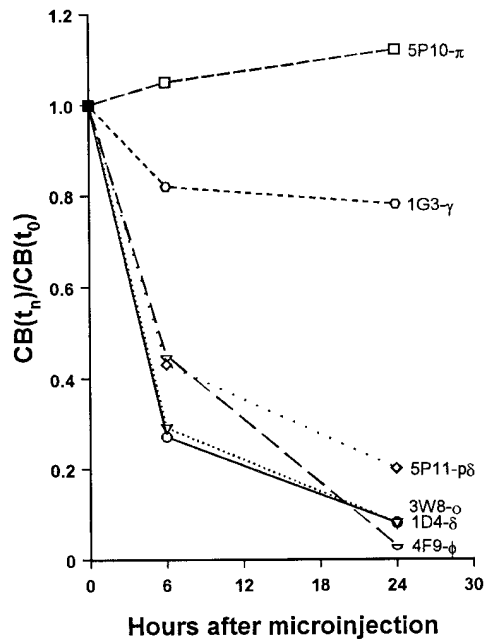


**Figure 6.** Quantitative analysis of the effects of mAb injection on coiled bodies. Cells were microinjected in the nucleus with mAbs  $\delta$ ,  $p\delta$ ,  $\gamma$ ,  $\pi$ ,  $\alpha$ , and  $\phi$ . The cells were either immediately permeabilized and fixed ( $t_0$ ), or further incubated for 6 or 24 h. The injected mAb was detected using fluorescein-conjugated secondary antibodies. Cells were double-labeled with a rabbit anti-coilin antiserum (204.3) detected using Texas red fluorescence. For each mAb, the percentage of injected cells with coiled bodies was estimated at each time point ( $CB[t_n]$ ), and the values at time zero ( $CB[t_0]$ ) were taken as reference. For each mAb, at least three independent microinjection experiments were performed. The total number of cells counted per mAb at each time point ranged between 100 and 600.

reveals intensely labeled coiled bodies, which do not appear to change their relative positions during the time-lapse observations (Fig. 7, A–F). Injection of the antibody in the cytoplasm is rapidly followed by transport to the nucleus and incorporation into coiled bodies (Fig. 7, A–D, arrows). Importantly, microinjected cells undergo mitosis (Fig. 7, C and F, arrowheads) and labeled coiled bodies are seen in the daughter cells (Fig. 7 E, arrows). This demonstrates that, first, microinjection is not perturbing normal cell physiology and, second, binding of mAb- $\pi$  to coilin is not preventing de novo assembly of coiled bodies.

In contrast with the above observations, injection of rhodamine-labeled mAb- $\delta$  into the nucleus shows a progressive disappearance of coiled bodies over a period of  $\sim$ 6 h (Fig. 8, A–G). However, coiled bodies are readily visible immediately after injection into the nucleus (Fig. 8 A) or shortly after injection into the cytoplasm (refer to Fig. 3 G). Thus, binding of mAb- $\delta$  is not preventing the assembly of coilin–antibody complexes into coiled bodies. Possibly, when complexes of mAb- $\delta$  with coilin are incorporated into a coiled body they block the subsequent assembly of new protein, leading to a progressive disappearance of the structure due to its normal turnover rate. Alternatively, the presence of mAb- $\delta$ /coilin complexes in a coiled body

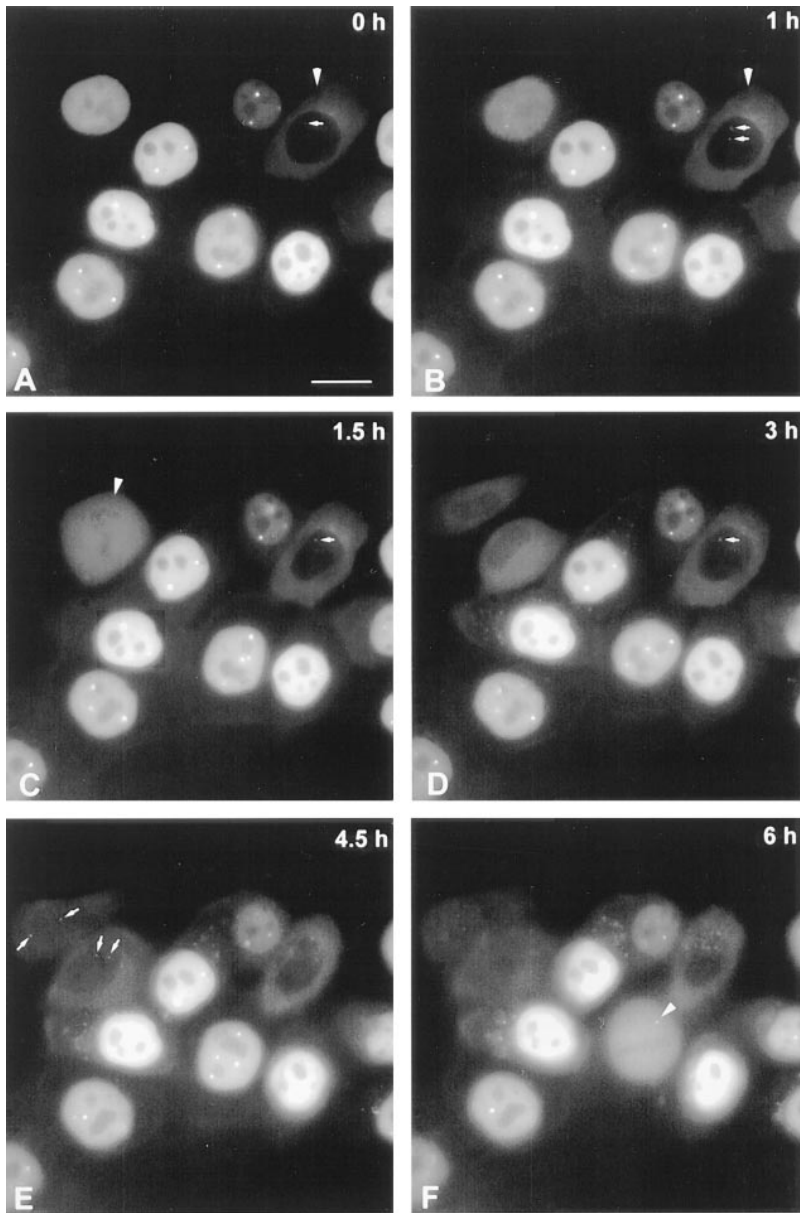


**Figure 7.** Analysis of mAb- $\pi$  in living cells. HeLa cells were injected with rhodamine-labeled mAb- $\pi$  and analyzed at 30-min intervals. All cells in this field were injected in the nucleus, except one that was injected in the cytoplasm (*A* and *B*, arrowheads). The time between injection and the first observation was  $\sim$ 20 min. Note that shortly after injection, the antibody injected in the cytoplasm (*A* and *B*, arrowheads) labels coiled bodies (*A–D*, arrows). At 1.5 h after the first observation, one cell initially injected in the nucleus has entered mitosis (arrowhead), and 3 h later coiled bodies are labeled in the daughter cell nuclei (*E*, arrows). At 6 h after the first observation, another cell is in mitosis and contains a labeled mitotic coiled body in the cytoplasm (*F*, arrowhead). Bar, 10  $\mu$ m.

may somehow trigger its disassembly. After their disappearance, coiled bodies are no longer visible in cells injected with mAb- $\delta$ , indicating that the antibody continues to exert its effect for a period of at least 39 h (Fig. 8, *H–L*). During this period, the injected cells remain viable, as shown by their ability to divide (Fig. 8, *K* and *L*, arrows).

Injection of rhodamine-labeled mAbs  $\sigma$  and  $\phi$  also produces a progressive disappearance of coiled bodies, whereas after injection of mAb- $\gamma$  coiled bodies remain visible, although they often appear to become smaller throughout the time-lapse analysis (data not shown).

Irrespective of the mAb used for injection, coiled bodies maintain their relative positions throughout the time-lapse observations. Although this would argue against the view that coiled bodies may act as carriers or transporters inside the nucleus, we cannot exclude that binding of the mAbs to coilin may exert an inhibitory effect on presumptive motion.

#### ***Coiled Body Disappearance Does Not Affect snRNP Localization or Nucleolar Structure***

Having established that intranuclear injection of mAbs promotes the disappearance of coiled bodies, we next asked how depriving a cell of the coiled body affects the subcellular distribution of splicing snRNPs. The U1, U2, U5, and U4/U6 snRNPs, all of which are localized in the coiled body, represent major components of the spliceosome. Each of these snRNPs is built of a unique species of snRNA associated with specific proteins. Additionally, all splicing snRNPs share a common set of proteins, termed the Sm proteins, that are tightly bound to the snRNAs (for review see Moore et al., 1993). During their biogenesis, the U1, U2, U4, and U5 snRNAs are transcribed in the nucleus and transported to the cytoplasm, where the Sm proteins bind. Thereafter, the assembled snRNP is imported to the nucleus (for review see Mattaj, 1988). In the nu-



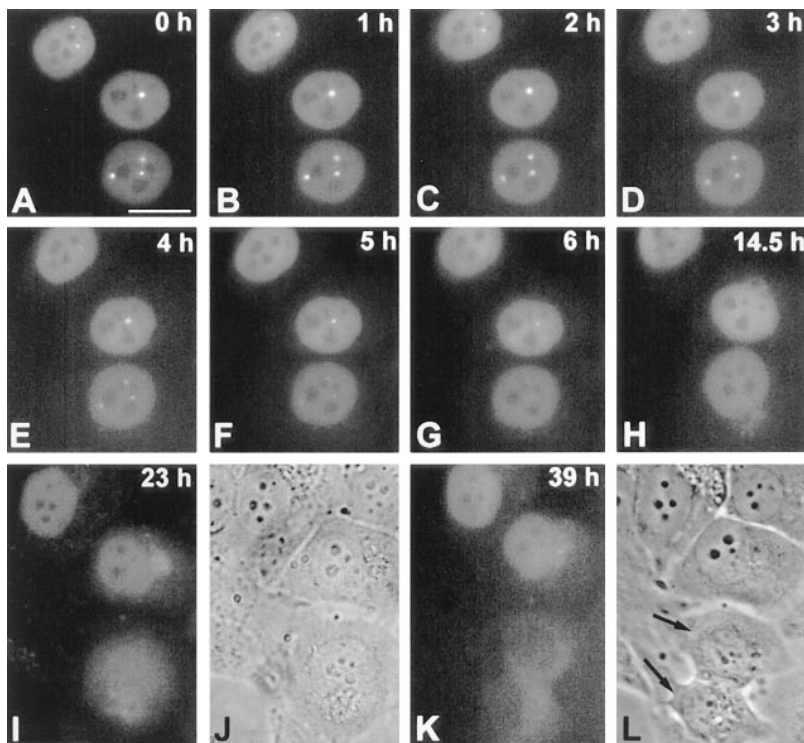


**Figure 8.** Analysis of mAb- $\delta$  in living cells. HeLa cells were injected with rhodamine-labeled mAb- $\delta$  and analyzed at 30-min intervals. All cells in this field were injected in the nucleus. The time between injection and the first observation was  $\sim$ 20 min. Within 6 h after the first observation, the coiled bodies progressively disappear (A–G). At later time points coiled bodies are never detected in these cells (H–L). Note that one of the cells has divided by 39 h (L, arrows). J and L depict phase-contrast images corresponding to I and K, respectively. Bar, 10  $\mu$ m.

nucleus, snRNPs are normally distributed throughout the nucleoplasm with additional concentration in interchromatin granules and coiled bodies (for review see Lamond and Carmo-Fonseca, 1993). To investigate whether the coiled body plays an important role in the subcellular distribution of snRNPs, cells were microinjected with mAb 1D4- $\delta$ , incubated for 24 h, fixed, and then double-labeled with either an antisense riboprobe specific for U2 snRNA (Fig. 9, A and B) or an antibody against the Sm proteins (Fig. 9, C and D). As depicted in the figure, no apparent change is observed in the distribution of either U2 snRNA or Sm protein in injected cells. Namely, there is no evidence for an accumulation of snRNA or Sm protein in the cytoplasm, and within the nucleus the distribution appears normal, except for the lack of accumulation at coiled bodies which is typically observed in noninjected cells (Fig. 9 B, arrows). Similar results were observed on cells microinjected with mAb 1D4- $\delta$  and incubated for 48 h before fixation and labeling (data not shown).

In a recent work, Bohmann and colleagues (1995a) reported that overexpression of mutated forms of the human p80 coilin gene induces a disorganization of both the coiled body and the nucleolus, suggesting that the two structures share either a common structural framework or a common assembly pathway. We therefore asked whether microinjection of antibodies that promote the disappearance of coiled bodies perturbs the organization of the nucleolus. Fig. 9, E and F depict a field of cells that were microinjected with mAb 1D4- $\delta$ , incubated for 48 h, fixed, and then double-labeled with a riboprobe specific for U3 snRNA. This small RNA associates with fibrillarin to form ribonucleoprotein particles that are normally localized in both the nucleolus and the coiled body. The results show that the distribution of U3 in injected cells is indistin-

guishable from that of noninjected cells. Similar results were observed using probes specific for other nucleolar components such as 28S rRNA and RNA polymerase I, after microinjection of three distinct mAbs that promote the disappearance of coiled bodies, namely 1D4- $\delta$ , 3W8-o, and 4F9- $\phi$  (data not shown). Since the structural organization of the nucleolus is strictly dependent upon ongoing biogenesis of rRNA (for review see Shaw and Jordan, 1995), the data strongly suggest that the disassembly of the coiled body is not affecting nucleolar function. Thus, microinjection of anti-coilin antibodies is specifically interfering with coiled bodies.

#### **Coiled Body Disappearance Does Not Impair Splicing of Pre-mRNAs**

Although the disappearance of coiled bodies induced by antibody microinjection does not alter the subnuclear distribution of spliceosomal snRNPs, we have further investigated whether it interferes with their metabolism and, consequently, with splicing. To perform these experiments we initially chose to infect cells with Ad2, and test the ability of injected cells to support splicing of the well-characterized viral major late pre-mRNA. Adenovirus contains a single major late promoter (MLP) that is strongly activated after the onset of viral replication, at  $\sim$ 8 h after infection, and attains maximal activity by 18 h after infection. The MLP encodes a large primary transcript that gives rise to five families of mRNAs (L1–L5) by differential splicing and polyadenylation (Sharp, 1984). Each of these mRNAs have in common a 5' noncoding region of 201 nucleotides, which is called the tripartite leader and is derived by the splicing of three small introns.

In a previous study we have shown that coiled bodies

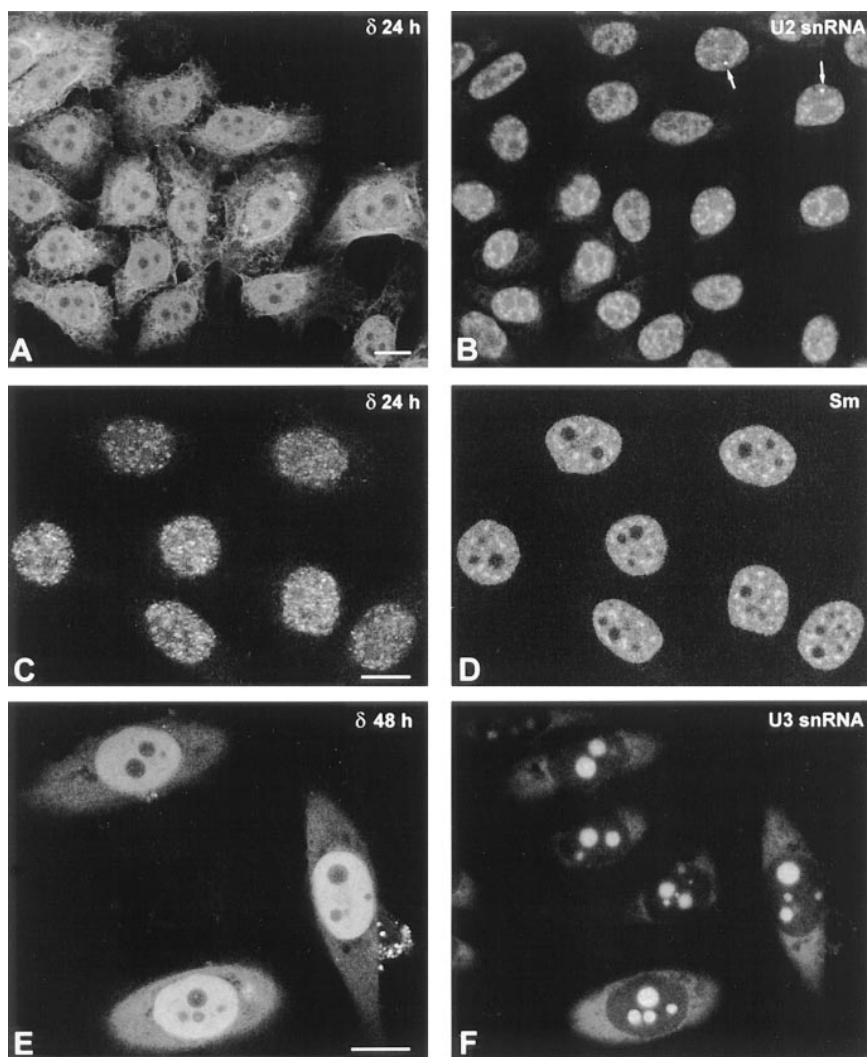


**Figure 9.** Coiled body disappearance does not affect snRNP localization. HeLa cells were microinjected with mAb- $\delta$  and incubated for either 24 (*A–D*) or 48 h (*E* and *F*) before fixation. The injected antibody was detected using a secondary antibody conjugated to Texas red (*A*, *C*, and *E*). The cells were double-labeled with either an antisense riboprobe specific for U2 snRNA (*B*), an antibody against the Sm proteins (*D*), or an antisense riboprobe specific for U3 snoRNA (*F*). Arrows in *B* point to U2 snRNA concentrated in the coiled bodies of noninjected cells. Bar, 10  $\mu$ m.

disassemble by 16–18 h of viral infection, most likely as a consequence of the block in host cellular protein synthesis induced by the virus (Rebello et al., 1996). However, coiled bodies are present during the early stages of Ad2 infection, suggesting that they might be required during the period of activation of viral late gene expression.

In this study, cells were microinjected with mAb 1D4- $\delta$ , incubated for either 6 or 24 h, and then infected with Ad2 for 18 h (Fig. 10, *A–D*). The cells were fixed and hybridized with an oligonucleotide probe complementary to the first splice junction of the tripartite leader (Bridge et al., 1996). To unambiguously identify cells that were simultaneously injected and infected, a triple-labeling experiment was performed using rhodamine to detect the injected mAb, Cy5 for the viral protein DBP (Linné et al., 1977), and fluorescein for spliced viral mRNA. As shown in Fig. 10, *A* and *B*, the hybridization signal produced by the splice junction probe is similar in injected (Fig. 10 *A*, arrow) and noninjected cells (Fig. 10 *A*, arrowheads). Similar results were observed on cells microinjected with mAb 1D4- $\delta$ , incubated for 24 h, and then infected with Ad2 for 18 h (Fig. 10, *C* and *D*). Similar results were also observed after injection of mAbs 3W8-o (which also promotes dis-

appearance of coiled bodies) and 5P10- $\pi$  (which does not disassemble coiled bodies; data not shown). Immunofluorescence analysis of injected cells using antibodies against the penton protein further confirmed that late viral gene expression was active in these cells (data not shown).

From these data we conclude that coiled bodies are not required to support either the early phase of infection (involving expression of a small number of proteins which prime the infected cell for the late phase) or the splicing of late viral mRNA.

Taking into account that viruses have evolved mechanisms to subvert the host cell machinery and that large amounts of partially spliced viral mRNAs accumulate in the nucleus of infected cells (Sharp, 1984), we next asked whether disappearance of coiled bodies affects splicing of a nonviral pre-mRNA. For this, HeLa cells were first coinjected with a transient expression vector carrying a human  $\beta$ -globin gene in the SV-40 episomal vector p $\beta$ SV328 (Grosveld et al., 1982) and an unspecific mouse IgG. After incubation for 6–24 h, the cells were fixed and double-labeled with an anti-mouse secondary antibody (to identify injected cells) and oligonucleotide probes complementary to either the first or the second splice junction of

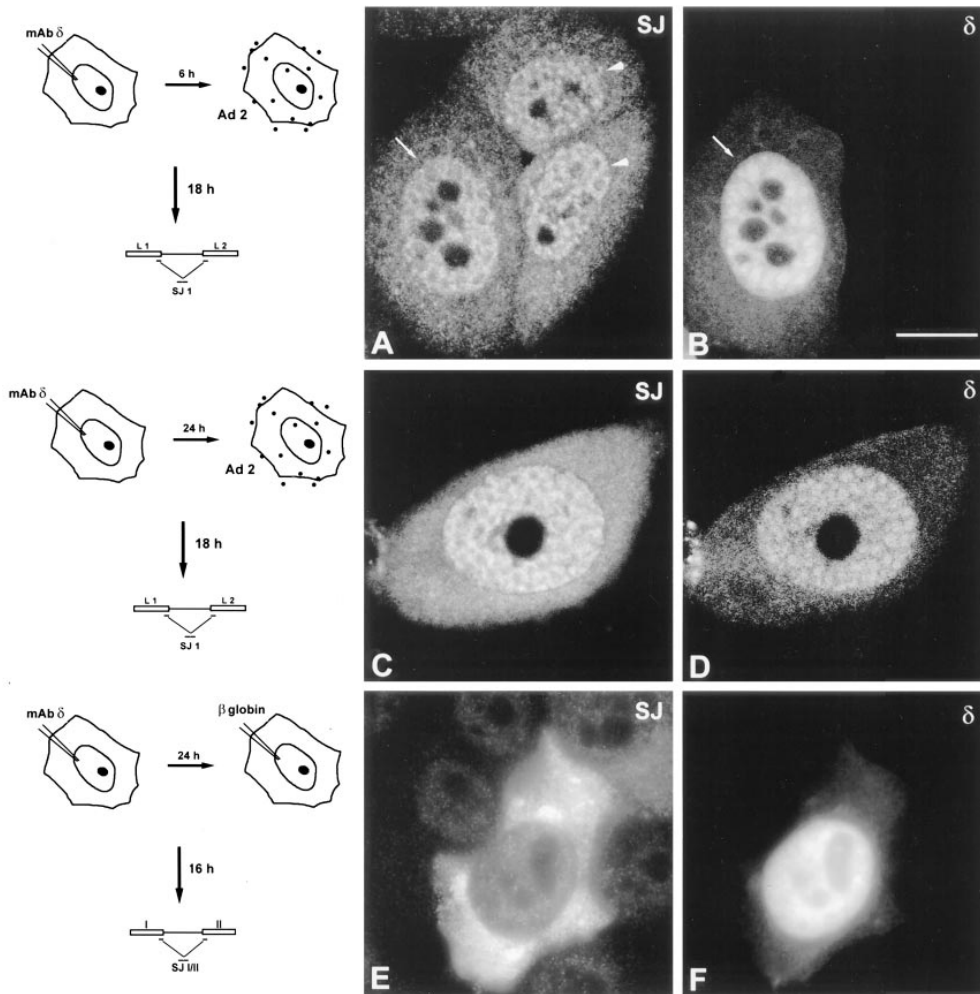


**Figure 10.** Coiled body disappearance does not impair splicing. (A–D) HeLa cells were microinjected with mAb- $\delta$ , incubated for either 6 (A and B) or 24 h (C and D) and then infected with Ad2 for 18 h. The cells were fixed and hybridized with an oligonucleotide probe complementary to the first splice junction of the tripartite leader (A and C). The injected antibody was detected using a secondary antibody conjugated to Texas red (B and D), and the viral protein DBP was detected using a secondary antibody conjugated to Cy5 (data not shown). The hybridization pattern in the injected cells (A, arrow; and C) is similar to that of noninjected cells (A, arrowheads). Note that in B and D, staining of the nucleoplasm is nonhomogeneous. This is due to the very intense signal produced by anti-DBP antibody, which is partially detected in the Texas red channel of the confocal microscope. (E and F) Cells were microinjected with mAb 1D4- $\delta$ , incubated for 24 h, and then re-injected with an expression plasmid carrying the human  $\beta$ -globin gene. The cells were fixed 16 h later

and hybridized with an oligonucleotide probe complementary to the first splice junction of  $\beta$ -globin mRNA (E). The injected antibody was detected using a secondary IgG conjugated to Texas red (F). Note that under the mild permeabilization conditions used here, the hybridization signal is predominantly detected in the cytoplasm. Bar, 10  $\mu$ m.

$\beta$ -globin mRNA (Custódio, N., M. Carmo-Fonseca, and M. Antoniou, unpublished data). From these experiments we concluded that maximal levels of spliced globin RNA were detected in the cytoplasm by 16 h after injection. Next, cells were injected with mAb- $\delta$ , incubated for 24 h, re-injected with  $\beta$ -globin plasmid DNA, and then further incubated for 16 h. The results obtained after hybridization using a probe complementary to the first splice junction of  $\beta$ -globin mRNA clearly indicate that the antibody-induced absence of coiled bodies is not preventing the accumulation of spliced  $\beta$ -globin mRNA in the cytoplasm (Fig. 10, E and F). Similar results were observed after hybridization using a probe complementary to the second splice junction of  $\beta$ -globin mRNA, or after injection of mAb-o (which also promotes disappearance of coiled bodies) and mAb- $\pi$  (which does not disassemble coiled bodies; data not shown).

In conclusion, the results show that high levels of splicing activity are taking place in nuclei devoid of coiled bodies.

## Discussion

### Microinjection of Anti-coilin Antibodies Induces the Disappearance of Coiled Bodies

We have demonstrated the feasibility of using anti-coilin antibodies to specifically interfere with the structure of coiled bodies in the nucleus of living cells. Monoclonal antibodies were raised against the coiled body protein p80-coilin, purified, and then microinjected into the nucleus of HeLa cells. Visualization was achieved by either staining of fixed cells or direct *in vivo* imaging using rhodamine-labeled antibody. The ability to carry out extended *in vivo* analysis was demonstrated by direct observation of injected cells undergoing cell division over a period of 24–48 h.

After microinjection into the nucleus, all mAbs labeled coiled bodies. Taking into account that a pool of intranuclear coilin is concentrated in coiled bodies and another pool is scattered throughout the nucleoplasm (refer to Fig.

3 A), this result may reflect either binding of the injected antibody to coilin molecules present in coiled bodies, or binding to nucleoplasmic coilin with subsequent assembly of antibody-coilin complexes into coiled bodies. The finding that coiled bodies become labeled upon microinjection of the antibody into the cytoplasm supports the latter interpretation, and it is possible that both mechanisms may occur when the antibody is injected into the nucleus.

Within 24 h after injection, two distinct antibody-induced phenotypes are clearly identified. The mAbs  $\delta$ ,  $\alpha$ , and  $\phi$  cause the disappearance of coiled bodies (as confirmed by double-labeling using an anti-coilin rabbit serum) in >90% of injected cells. In contrast, mAb- $\pi$  has no apparent effect on the integrity of the coiled body and mAb- $\gamma$  induces only a slight decrease (<20%) in the number of cells with coiled bodies. Most probably, the first phenotype is caused by the fact that antibody-coilin complexes incorporated in a coiled body impair the subsequent assembly of new coilin molecules. This may either directly trigger disassembly of the structure or simply lead to its disappearance as a consequence of its high turnover rate. In fact, two lines of evidence suggest that the coiled body goes through a rapid cycle of assembly/disassembly in the nucleus. First, exogenous coilin is able to correctly localize in coiled bodies, although overexpression of the protein fails to increase their size or number (Wu et al., 1994; Bohmann et al., 1995a). Second, treatment of cells with inhibitors of protein synthesis causes a progressive disappearance of coiled bodies (Lafarga et al., 1994; Rebelo et al., 1996).

Remarkably, the mAbs capable of interfering with the coiled body bind to epitopes spread throughout the coilin protein (refer to Fig. 2). In good agreement with this, it was previously reported that removal of either amino- or carboxy-terminal sequences of p80-coilin prevented interaction with coiled bodies (Bohmann et al., 1995a). Taken together, these data suggest that assembly of coilin into coiled bodies requires multiple sequence motifs scattered along the protein.

### *Coiled Body Disappearance Does Not Impair Splicing*

Currently proposed hypothesis for the function of the coiled body are based on the idea that this structure is somehow involved in snRNP metabolism (see Bohmann et al., 1995b). According to the model that snRNPs must cycle through the coiled body in order to be recycled, assembled or modified de novo, one prediction would be that in the absence of coiled bodies either preexisting or newly synthesized snRNPs would become unavailable for spliceosome assembly. Although slow proliferating cells such as primary human fibroblasts are normally devoid of coiled bodies (Huang and Spector, 1992), they contain coilin and may assemble coiled bodies (Carmo-Fonseca et al., 1993). Possibly, in the presence of low levels of splicing activity the requirements for snRNP recycling or de novo synthesis are so low that coiled bodies form only transiently or are too small to be clearly identified with the light microscope. Consistent with this view, coiled bodies are conspicuous in metabolically activate cells and become more numerous upon stimulation of gene expression (Ochs et al., 1995). Therefore, to determine whether the

disappearance of coiled bodies affects snRNP function, it is important to overload the nucleus with highly abundant intron-containing transcripts. Furthermore, taking into account that the half-lives of spliceosomal snRNPs are  $\sim 20$  h (Moore et al., 1993), it is crucial to analyze cells devoid of coiled bodies for long periods of time.

Here we have microinjected mAbs that induce disappearance of coiled bodies, incubated the cells for 24 h, and then infected them with adenovirus. The human Ad2 causes a productive infection of HeLa cells that proceeds through an infectious cycle of  $\sim 36$  h (for review see Horwitz, 1990). This cycle is conventionally divided into early and late stages, separated by the onset of viral replication which occurs at  $\sim 8$  h after infection. After the onset of viral DNA replication,  $\sim 90\%$  of the genome is expressed and the amount of RNA made increases up to 10-fold. During this phase a single MLP is strongly activated and encodes a large primary transcript that gives rise to five families of mRNAs (L1–L5) by differential splicing and polyadenylation (Sharp, 1984). Each of these mRNAs have in common a 5' noncoding region of 201 nucleotides, which is called the tripartite leader and is derived by the splicing of three small introns. Transcription from MLP attains a maximum level at 18 h after infection and then remains constant for at least 10 h, yielding large amounts of structural polypeptides that comprise the virion particle or are involved in packaging viral genomic DNA. During this period, the viruses compete with the host cell for control of the translational apparatus and Ad2 has evolved multiple mechanisms that suppress cellular protein synthesis and enhance translation of late viral mRNAs. Probably as a consequence of the block of host protein synthesis, most coiled bodies disassemble by 16–18 h of viral infection (Rebelo et al., 1996). However, coiled bodies are present during the early stages of Ad2 infection and it remained an open issue whether they are required during that period. The data presented here indicate that disappearance of coiled bodies does not impair either early or late phases of adenoviral infection. In fact, cells that were infected as long as 24 h after microinjection of mAbs contain high amounts of spliced tripartite leader mRNAs in the cytoplasm and express normal levels of late phase proteins.

In another set of experiments we analyzed the effect of antibody-induced disassembly of coiled bodies on splicing of transiently overexpressed  $\beta$ -globin transcripts. Control experiments show that within 16 h after plasmid injection there is an intense cytoplasmic hybridization signal produced by a splice junction probe, indicating that these cells are splicing large amounts of  $\beta$ -globin pre-mRNAs. Remarkably, cells that were injected with mAb- $\delta$ , incubated for 24 h, and then reinjected with  $\beta$ -globin expression vector continue to splice and export  $\beta$ -globin mRNA to the cytoplasm. Thus, highly abundant pre-mRNAs continue to be spliced in the absence of coiled bodies. However, due to the long half-lives of spliceosomal snRNPs, it is possible that during the time course of our experiments the level of preexisting snRNPs available in the nucleus does not drop below the threshold required to maintain splicing activity.

Although the data presented here do not exclude the hypothesis that coiled bodies play a basic role in snRNP biogenesis or recycling, alternative ideas should be considered concerning the function of this structure. First, the

coiled body may simply represent a storage site for snRNPs in the nucleus. However, we find this hypothesis unlikely taking into account that coiled bodies are very dynamic structures strictly dependent upon ongoing RNA and protein synthesis (Carmo-Fonseca et al., 1992; Lafarga et al., 1994; Rebelo et al., 1996). Second, coiled bodies may be involved in some type of protein or snRNA modification that is not essential for splicing. For instance, it is known that snRNAs undergo extensive posttranscriptional modifications on base and sugar residues, and it was recently proposed that these modifications could be introduced into snRNA at the coiled body, by the same (or similar) enzymatic machinery that is used in the nucleolus to modify rRNA (Bohmann et al., 1995b). Very little is known about the functional significance of these modifications in the U1, U2, U5, and U4/U6 snRNPs, and therefore it is conceivable that at least some may not be essential for spliceosome assembly. Third, coiled bodies may be preferentially involved in the metabolism of specialized RNAs in differentiated tissue cells such as neurons. Finally, it is important to consider that coiled bodies, like nucleoli, may represent the morphological consequence of an activity that does not necessarily require a dedicated compartment in the nucleus. In fact, one may argue that the nucleolus as an organized preassembled structure is not essential for ribosome biogenesis, since processing of ribosomal RNA occurs normally when expressed from a plasmid containing a single copy of the rRNA gene (Nierras et al., 1997). Here we observe that upon disassembly of the coiled body by antibody injection, the pool of coilin dispersed throughout the nucleoplasm is intensified (refer to Fig. 4). Thus, it is possible that whatever activity is taking place at the coiled body it may also occur in association with nucleoplasmic coilin. Consistent with this view, it was recently reported that coiled bodies tend to associate preferentially with tandem repeated or tightly clustered genes, suggesting that, like nucleoli and rRNA genes, the coiled body may arise as a local concentration of p80-coilin determined by expression of these clustered genes (Gao et al., 1997). In conclusion, it will be important for future experiments addressing the function of the coiled body to focus on suppressing the expression of p80-coilin at both cell and organism level.

We wish to acknowledge D. Ferreira (University of Lisbon, Lisbon, Portugal) and A. Lamond (University of Dundee, Dundee, UK) for support. We are also grateful to A. Sawyer (European Molecular Biological Laboratory [EMBL], Heidelberg, Germany) for extensive technical advice on monoclonal antibody production, to J. Romão (Gulbenkian Institute, Qeiras, Portugal) for animal care facilities, and to our colleagues M. Carvalho, N. Custódio, and L. Teixeira (all three from University of Lisbon) for help in some experiments and for critical discussions. We thank the following groups for generously providing materials used in this study: A. Lamond and K. Bohmann (EMBL) for p80-coilin cDNAs, anti-coilin rabbit serum 204.3, and U2 snRNA riboprobe; E. Bridge (University of Uppsala, Uppsala, Sweden) for adenoviruses, splice-junction probe, anti-DBP, and antipenton antibodies; M. Antoniou (Guy's Hospital, London, UK) for  $\beta$ -globin expression vector and splice-junction probes; and W. van Venrooij (University of Nijmegen, Nijmegen, The Netherlands) for anti-Sm autoimmune serum C45.

This study was supported by grants from Junta Nacional de Investigação Científica e Tecnológica/Program PRAXIS XXI and from the European Union. F. Almeida was supported by a PRAXIS XXI doctoral fel-

lowship and a short-term fellowship from the European Molecular Biology Organization.

Received for publication 2 March 1998 and in revised form 26 June 1998.

## References

- Andrade, L.E.C., E.K.L. Chan, I. Raska, C.L. Peebles, G. Roos, and E.M. Tan. 1991. Human autoantibody to a novel protein of the nuclear coiled body: immunological characterization and cDNA cloning of p80-coilin. *J. Exp. Med.* 173:1407-1419.
- Ansorge, W., and R. Pepperkok. 1988. Performance of an automated system for capillary microinjection into living cells. *J. Biochem. Biophys. Methods.* 16: 283-292.
- Bauer, D.W., C. Murphy, Z. Wu, C.-H.H. Wu, and J.G. Gall. 1994. In vitro assembly of coiled bodies in *Xenopus* egg extracts. *Mol. Biol. Cell.* 5:633-644.
- Beven, A.F., G.G. Simpson, J.W.S. Brown, and P.J. Shaw. 1995. The organization of spliceosomal components in the nuclei of higher plants. *J. Cell Sci.* 108:509-518.
- Bohmann, K., J. Ferreira, and A.I. Lamond. 1995a. Mutational analysis of p80 coilin indicates a functional interaction between coiled bodies and the nucleolus. *J. Cell Biol.* 131:817-831.
- Bohmann, K., J. Ferreira, N. Santama, K. Weis, and A.I. Lamond. 1995b. Molecular analysis of the coiled body. *J. Cell Sci.* 19(Suppl.):107-113.
- Borer, R.A., C.F. Lehner, H.M. Eppenberger, and E.A. Nigg. 1989. Major nucleolar proteins shuttle between nucleus and cytoplasm. *Cell.* 56:379-390.
- Bridge, E., K.-U. Riedel, B.-M. Johansson, and U. Pettersson. 1996. Spliced exons of adenovirus late RNAs colocalize with snRNP in a specific nuclear domain. *J. Cell Biol.* 135:303-314.
- Bruck, C., D. Portetelle, C. Glineur, and A. Bollen. 1982. One-step purification of mouse monoclonal antibodies from ascitic fluid by DEAE Affi-Gel Blue chromatography. *J. Immunol. Methods.* 53:313-319.
- Carmo-Fonseca, M., D. Tollervey, R. Pepperkok, S.M.L. Barabino, A. Merdes, C. Brunner, P.D. Zamore, M.R. Green, E.C. Hurt, and A.I. Lamond. 1991a. Mammalian nuclei contain foci which are highly enriched in components of the pre-mRNA splicing machinery. *EMBO (Eur. Mol. Biol. Organ.) J.* 10: 195-206.
- Carmo-Fonseca, M., R. Pepperkok, B.S. Sproat, W. Ansorge, M.S. Swanson, and A.I. Lamond. 1991b. In vivo detection of snRNP-organelles in the nuclei of mammalian cells. *EMBO (Eur. Mol. Biol. Organ.) J.* 10:1863-1873.
- Carmo-Fonseca, M., R. Pepperkok, M.T. Carvalho, and A.I. Lamond. 1992. Transcription-dependent colocalization of the U1, U2, U4/U6, and U5 snRNPs in coiled bodies. *J. Cell Biol.* 117:1-14.
- Carmo-Fonseca, M., J. Ferreira, and A.I. Lamond. 1993. Assembly of snRNP-containing coiled bodies is regulated in interphase and mitosis: evidence that the coiled body is a kinetic nuclear structure. *J. Cell Biol.* 120:841-852.
- Carmo-Fonseca, M., K. Bohmann, M.T. Carvalho, and A.I. Lamond. 1994. P80-coilin. In *Manual of Biological Markers of Disease*. W.J. van Venrooij and R.N. Maini, editors. Kluwer Academic Publishers, Norwell, MA. B8.2:1-11.
- Chan, E.K.L., S. Takano, L.E.C. Andrade, J.C. Hamel, and A.G. Matera. 1994. Structure, expression, and chromosomal localization of human p80-coilin gene. *Nucl. Acids Res.* 22:4462-4469.
- Fey, E.G., G. Krochmalnic, and S. Penman. 1986. The nonchromatin substructures of the nucleus: the ribonucleoprotein (RNP)-containing and RNP-depleted matrices analyzed by sequential fractionation and resinless section electron microscopy. *J. Cell Biol.* 102:1654-1665.
- Frey, M.R., and A.G. Matera. 1995. Coiled bodies contain U7 small nuclear RNA and associate with specific DNA sequences in interphase human cells. *Proc. Natl. Acad. Sci. USA.* 92:5915-5919.
- Gall, J.G., A. Tsvetkov, Z. Wu, and C. Murphy. 1995. Is the sphere organelle/coiled body a universal nuclear component? *Dev. Genet.* 16:25-35.
- Gama-Carvalho, M., R.D. Kraus, L. Chiang, J. Valcárcel, M.R. Green, and M. Carmo-Fonseca. 1997. Targeting of U2AF65 to sites of active splicing in the nucleus. *J. Cell Biol.* 137:975-987.
- Gao, L., M.R. Frey, and A.G. Matera. 1997. Human genes encoding U3 snRNA associate with coiled bodies in interphase cells and are clustered on chromosome 17p11.2 in a complex inverted repeat structure. *Nucleic Acids Res.* 25: 4740-4747.
- Grosveld, F., E. de Boer, C.K. Shewmaker, and R.A. Flavell. 1982. DNA sequences necessary for transcription of the rabbit beta-globin gene in vivo. *Nature.* 295:120-126.
- Harlow, E., and D. Lane. 1988. *Antibodies: A Laboratory Manual*. Cold Spring Harbor Laboratory Press, Cold Spring Harbor, NY. 726 pp.
- Hardin, J.W., S.S. Spicer, and W.B. Green, editors. 1969. The paranucleolar structure, accessory body of Cajal, sex chromatin, and related structures in nuclei of rat trigeminal neurons: a cytochemical and ultrastructural study. *Anat. Rec.* 164:403-432.
- Hervás, J.P., J. Villegas, D. Crespo, and M. Lafarga. 1980. Coiled bodies in supraoptic nucleus of the rat hypothalamus during the postnatal period. *Am. J. Anat.* 159:447-454.
- Herr, S., T. Bastian, R. Pepperkok, C. Boulin, and W. Ansorge. 1993. A fully automated image acquisition and analysis system for low light level fluorescence microscopy. *Methods Mol. Cell. Biol.* 4:164-170.

- Horwitz, M.S. 1990. Adenoviridae and Their Replication. In *Virology*. Vol. 1, B.N. Fields and D.M. Knipe, editors. Raven Press, New York. 1679–1721.
- Huang, S., and D.L. Spector. 1992. U1 and U2 small nuclear RNAs are present in nuclear speckles. *Proc. Natl. Acad. Sci. USA*. 89:305–308.
- Huang, S., T.J. Deerinck, M.H. Ellisman, and D.L. Spector. 1994. In vivo analysis of the stability and transport of nuclear poly(A)<sup>+</sup> RNA. *J. Cell Biol.* 126:877–899.
- Jiménez-García, L.F., M.L. Segura-Valdez, R.L. Ochs, L.I. Rothblum, R. Hannan, and D.L. Spector. 1994. Nucleogenesis: U3 snRNA-containing pre-nucleolar bodies move to sites of active pre-rRNA transcription after mitosis. *Mol. Biol. Cell*. 5:955–966.
- Jordan, P., M. Mannervik, L. Tora, and M. Carmo-Fonseca. 1996. In vivo evidence that TATA-binding protein/SL1 colocalizes with UBF and RNA polymerase I when rRNA synthesis is either active or inactive. *J. Cell Biol.* 133:225–234.
- Jordan, P., C. Cunha, and M. Carmo-Fonseca. 1997. The cdk7-cyclinH-MAT1 complex associated with TFIIF is localized in coiled bodies. *Mol. Biol. Cell*. 8:1207–1217.
- Lafarga, M., M.T. Berciano, M.A. Andres, and P.S. Testillano. 1994. Effects of cycloheximide on the structural organization of the nucleolus and the coiled body in normal and stimulated supraoptic neurons of the rat. *J. Neurocytol.* 23:500–513.
- Lamond, A.I., and M. Carmo-Fonseca. 1993. The coiled body. *Trends Cell Biol.* 3:198–204.
- Linné, T.H., H. Jornvall, and L. Philipson. 1977. Purification and characterization of the phosphorylated DNA binding protein from adenovirus type 2 infected cells. *Eur. J. Biochem.* 76:481–490.
- Lyon, C.E., K. Bohmann, J. Sleeman, and A.I. Lamond. 1997. Inhibition of protein dephosphorylation results in the accumulation of splicing snRNPs and coiled bodies within the nucleolus. *Exp. Cell Res.* 230:84–93.
- Mattaj, I.W. 1988. U snRNP assembly and transport. In *Structure and Function of Major and Minor Small Nuclear Ribonucleoprotein Particles*. M. Birnstiel, editor. Springer Verlag, New York. 100–114.
- Meier, U.T., and G. Blobel. 1994. NAP57, a mammalian nucleolar protein with a putative homolog in yeast and bacteria. *J. Cell Biol.* 127:1505–1514.
- Monneron, A., and W. Bernhard. 1969. Fine structural organization of the interphase nucleus in some mammalian cells. *J. Ultrastruct. Res.* 27:266–288.
- Moore, M.J., C.C. Query, and P. Sharp. 1993. Splicing of precursors to mRNA by the spliceosome. In *The RNA World*. Cold Spring Harbor Laboratory Press, Cold Spring Harbor, NY. 303–357.
- Moreno Diaz de la Espina, S., A. Sanchez Pina, M.C. Risueño, F.J. Medina, and M.E. Fernandez-Gomes. 1980. The role of plant coiled bodies in the nuclear RNA metabolism. *Electron Microsc.* 2:240–241.
- Nierras, C.R., S.W. Liebman, and J.R. Warner. 1997. Does *Saccharomyces* need an organized nucleolus? *Chromosoma*. 105:444–451.
- Ochs, R.L., T.W. Stein, Jr., L.E.C. Andrade, D. Gallo, E.K.L. Chan, E.M. Tan, and K. Brasch. 1995. Formation of nuclear bodies in hepatocytes of estrogen-treated roosters. *Mol. Biol. Cell*. 6:345–356.
- Ramón y Cajal, S.R. 1903. Un sencillo método de coloración selectiva del retículo protoplásmico y sus efectos en los diversos órganos nerviosos de vertebrados e invertebrados. *Trab. Lab. Invest. Biol.* 2:129–221.
- Raska, I., R.L. Ochs, L.E.C. Andrade, E.K.L. Chan, R. Burlingame, C. Peebles, D. Gruol, and E.M. Tan. 1990. Association between the nucleolus and the coiled body. *J. Struct. Biol.* 104:120–127.
- Raska, I., L.E.C. Andrade, R.L. Ochs, E.K.L. Chan, C.-M. Chang, G. Roos, and E.M. Tan. 1991. Immunological and ultrastructural studies of the nuclear coiled body with autoimmune antibodies. *Exp. Cell Res.* 195:27–37.
- Rebelo, L., F. Almeida, C. Ramos, K. Bohmann, A.I. Lamond, and M. Carmo-Fonseca. 1996. The dynamics of coiled bodies in the nucleus of adenovirus-infected cells. *Mol. Biol. Cell*. 7:1137–1151.
- Roth, M.B. 1995. Spheres, coiled bodies and nuclear bodies. *Curr. Opin. Cell Biol.* 7:325–328.
- Sharp, P.A. 1984. Adenovirus transcription. In *The Adenovirus*. H.S. Ginsberg, editor. Plenum Press, New York. 173–204.
- Shaw, P.J., and E.G. Jordan. 1995. The nucleolus. *Annu. Rev. Cell Dev. Biol.* 11:93–121.
- Tuma, R.S., J.A. Stolk, and M.B. Roth. 1993. Identification and characterization of a sphere organelle protein. *J. Cell Biol.* 122:767–773.
- Wu, Z., C. Murphy, C.-H.H. Wu, A. Tsvetkov, and J.G. Gall. 1993. Snurposomes and coiled bodies. *Cold Spr. Harb. Symp. Quant. Biol.* 58:747–754.
- Wu, Z., C. Murphy, and J.G. Gall. 1994. Human p80-coilin is targeted to sphere organelles in the amphibian germinal vesicle. *Mol. Biol. Cell*. 5:1119–1127.
- Yannoni, Y.M., and K. White. 1997. Association of the neuron-specific RNA binding domain-containing protein ELAV with the coiled body in *Drosophila* neurons. *Chromosoma*. 105:332–341.
- Zhang, G., K.L. Taneja, R.H. Singer, and M.R. Green. 1994. Localization of pre-mRNA splicing in mammalian nuclei. *Nature*. 372:809–812.